noted. This research was supported by the Director, Office of Energy Research, Office of Basic Energy Sciences, Chemical Sciences Division of the U.S. Department of Energy under Contract no. DE-AC03-76SF00098. C.B.M. thanks the Miller Institute for Basic Research in Science at the University of California, Berkeley, for a Research Professorship (1987–88); E.P.W. acknowledges a predoctoral fellowship from the National Science Foundation.

Registry No. 1, 12078-25-0; **2**, 73740-50-8; **3**, 77674-12-5; **4**, 73740-48-4; **5**, 53450-14-9; CpCo(CO)(C_4H), 115462-20-9; CpCo(CO)(η^2-C_6H_6), 115462-21-0; CpCo(CO)(THF), 115462-22-1; CpCo(CO)(CH_3CN), 115462-23-2; CpCo(CO)(P(n-Bu)$_3$), 87145-23-1; P(n-Bu)$_3$, 603-35-0; CH_3CN, 75-05-8; N_2, 7727-37-9; CO, 630-08-0; C_2H_4, 74-85-1.

Ground Spin State Variability in $[Fe_4S_4(SR)_4]^{3-}$. Synthetic Analogues of the Reduced Clusters in Ferredoxins and Other Iron–Sulfur Proteins: Cases of Extreme Sensitivity of Electronic State and Structure to Extrinsic Factors

M. J. Carney,[1a] G. C. Papaefthymiou,[1b] K. Spartalian,[1c] R. B. Frankel,[1b,d] and R. H. Holm*[,1a]

Contribution from the Department of Chemistry, Harvard University, Cambridge, Massachusetts 02138, and the Francis Bitter National Magnet Laboratory, Massachusetts Institute of Technology, Cambridge, Massachusetts 02139.

Received February 29, 1988

Abstract: A discovery of considerable significance in the field of synthetic and biological iron–sulfur clusters is the existence of ground states of different spin multiplicities for reduced tetranuclear clusters containing the $[4Fe\text{–}4S/Se]^+$ core. In addition to the conventional $S = {}^1/_2$ ground state, states with $S = {}^3/_2$, ${}^5/_2$, and ${}^7/_2$ have been identified in proteins and enzymes. We have recently demonstrated the existence of the $S = {}^3/_2$ state in completely characterized compounds containing $[Fe_4S_4(SR)_4]^{3-}$ as the synthetic analogue of native clusters. In this work the electronic properties of some 16 compounds containing 13 different clusters have been examined by Mössbauer and EPR spectroscopy and by determination of magnetization behavior and magnetic susceptibilities. Three categories of ground spin state behavior have been identified: (i) pure spin $S = {}^1/_2$ or ${}^3/_2$; (ii) physical mixtures of $S = {}^1/_2$ and ${}^3/_2$ states; and (iii) spin-admixed ground states ($S = {}^1/_2 + {}^3/_2$). Category (i) is recognized by Curie behavior and saturation magnetization at low temperatures and by characteristic magnetic Mössbauer and EPR spectra. Of all compounds examined, only one is a pure $S = {}^1/_2$ cluster; this spin state appears to be common in proteins. Category (ii) clusters exhibit intermediate Curie constants and saturation magnetization values and composite EPR and Mössbauer spectra. Category (iii) clusters are primarily distinguished by the absence of EPR and Mössbauer features from $S = {}^1/_2$ and ${}^3/_2$ clusters. Synthetic and native clusters show substantial similarities in a given spin state; the properties of the former, which are unambiguously characterized, fully support spin state assignments of the latter. Regardless of their occurrence in these categories, all polycrystalline cluster compounds when dissolved and frozen in DMF or acetonitrile exist as physical mixtures of $S = {}^1/_2$ and ${}^3/_2$ spin states. No biological example of a spin-admixed cluster has yet been identified. It is shown that the fine details of cluster structure and accompanying stabilization of a ground spin state are highly sensitive to environment. The structures of all $[Fe_4S_4(SR)_4]^{3-}$ clusters, which show a variety of distortions from idealized cubic symmetry, are summarized and spin state–structure correlations are explored. It is concluded that, at least from structures determined at room temperature, there is no strong relationship between core structure or terminal ligand conformation and spin state. The collective results make entirely clear, by means of its responsiveness to exogenous factors, the stereochemical "softness" of the core structure which, for both synthetic and native clusters and in conjunction with ligand conformation, is doubtless of importance in stabilizing different ground spin states.

Ongoing research in this laboratory[2-12] has demonstrated that the reduced synthetic clusters $[Fe_4S_4(SR)_4]^{3-}$ manifest a structural and spin-state variability that has no parallel in the chemistry of the oxidized clusters $[Fe_4S_4(SR)_4]^{2-}$. These di- and trianionic clusters possess the cubane-type core units $[4Fe\text{–}4S]^{2+}$ and $[4Fe\text{–}4S]^+$, respectively, which are isoelectronic with cluster cores in oxidized and reduced ferredoxins (Fd) and other iron–sulfur proteins. In particular, we have recently shown that some of these reduced clusters exist in different spin ground states, $S = {}^1/_2$[11] or ${}^3/_2$,[11,12] which are exclusively occupied at very low temperatures.

It is becoming increasingly clear that biological clusters at the $[4Fe\text{–}4S]^+$ oxidation level can also deviate from what has long

---

[1] (a) Harvard University. (b) Massachusetts Institute of Technology. (c) Department of Physics, University of Vermont. (d) Current address: Department of Physics, California Polytechnic State University, San Luis Obispo, CA 93407.

[2] Berg, J. M.; Holm, R. H. In *Metals Ions in Biology*; Spiro, T. G., Ed.; Interscience: New York, 1982; Vol. 4, Chapter 1.

[3] Cambray, J.; Lane, R. W.; Wedd, A. G.; Johnson, R. W.; Holm, R. H. *Inorg. Chem.* **1977**, *16*, 2656.

[4] Reynolds, J. G.; Laskowski, E. J.; Holm, R. H. *J. Am. Chem. Soc.* **1978**, *100*, 5315.

[5] Laskowski, E. J.; Frankel, R. B.; Gillum, W. O.; Papaefthymiou, G. C.; Renaud, J.; Ibers, J. A.; Holm, R. H. *J. Am. Chem. Soc.* **1978**, *100*, 5322.

[6] Berg, J. M.; Hodgson, K. O.; Holm, R. H. *J. Am. Chem. Soc.* **1979**, *101*, 4586.

[7] Laskowski, E. J.; Reynolds, J. G.; Frankel, R. B.; Foner, S.; Papethymiou, G. C.; Holm, R. H. *J. Am. Chem. Soc.* **1979**, *101*, 6562.

[8] Reynolds, J. G.; Coyle, C. L.; Holm, R. H. *J. Am. Chem. Soc.* **1980**, *102*, 4350.

[9] Stephan, D. W.; Papefthymiou, G. C.; Frankel, R. B.; Holm, R. H. *Inorg. Chem.* **1983**, *22*, 1550.

[10] Hagen, K. S.; Watson, A. D.; Holm, R. H. *Inorg. Chem.* **1984**, *23*, 2984.

[11] Carney, M. J.; Holm, R. H.; Papaefthymiou, G. C.; Frankel, R. B. *J. Am. Chem. Soc.* **1986**, *108*, 3519.

[12] Carney, M. J.; Papaefthymiou, G. C.; Whitener, M. A.; Spartalian, K.; Frankel, R. B.; Holm, R. H. *Inorg. Chem.* **1988**, *27*, 346.

0002-7863/88/1510-6084$01.50/0

been believed to be the usual (or only) ground state, viz., $S = {}^1/_2$, with its characteristic EPR and Mössbauer spectroscopic properties. Among leading examples are the $[4Fe-4Se]^+$ clusters in selenium-reconstituted clostridial Fds studied by Meyer and coworkers,[13-20] the $[4Fe-4S]^+$ center of the Fe protein of *Azotobacter vinelandii* nitrogenase (*Av2*), whose spectroscopic features under a variety of solvent and nucleotide binding conditions have been examined in detail by Lindahl et al.,[21,22] and the reduced Fe protein from the alternative (vanadium-containing) nitrogenase studied by Hales et al.[23] Each of these proteins exists as a mixture of (at least) $S = {}^1/_2$ and ${}^3/_2$ states, with the proportion of the two dependent on the medium and chemical state of the protein. In addition, EPR and Mössbauer spectroscopic evidence suggests that certain $[4Fe-4Se]^+$ clusters in $Se-Fd_{red}$[17-20] and the $[4Fe-4S]^+$ cluster in ATP-bound *Av2*[22] populate states with $S > {}^3/_2$.

Given the fundamental nature of the spin ground state in interpreting virtually all spectroscopic features of synthetic and native clusters, and its possible relation to their structures, reactivities, and redox potentials, we have substantially expanded our investigation of the variability of this property in reduced clusters. In this report, we provide a detailed comparison of the magnetic susceptibility, magnetization, EPR, and Mössbauer spectroscopic features of pure $S = {}^1/_2$ and ${}^3/_2$ clusters that are synthetic analogues of native clusters. Further, we show that certain analogues as polycrystalline solids appear to exist as physical mixtures of pure spin states, while others cannot be interpreted in this manner and are better described as constituting a new class of "spin-admixed" clusters. Finally, we present evidence that all analogue clusters in solution are in fact mixtures of clusters in doublet and quartet spin states.

Experimental Section

Preparation of Compounds. All manipulations were carried out under a pure dinitrogen or dinitrogen/helium atmosphere. Solvents were thoroughly dried and degassed before use. The following compounds were prepared as previously described, using the single-step synthesis of reduced clusters[10] or the reduction of $[Fe_4S_4(SR)_4]^{2-}$ with sodium acenaphthylenide[3] in acetonitrile solution: $(Et_3NMe)_3[Fe_4S_4(SPh)_4]$,[5] $(Et_4N)_3[Fe_4S_4(SCH_2Ph)_4]$,[3] $(Et_4N)_3[Fe_4S_4(S\text{-}p\text{-}C_6H_4Br)_4]$,[9] $(Et_4N)_3[Fe_4S_4(SR)_4]$ (R = Me, Et, *i*-Pr[10]), $(Et_4N)_3[Fe_4S_4(S\text{-}t\text{Bu})_4]\cdot MeCN$,[10] $(Et_4N)_3[Fe_4S_4(SC_6H_{11})_4]\cdot 4MeCN$,[11] and $(Me_4N)_3[Fe_4X_4(SPh)_4]\cdot 2MeCN$ (X = S, Se[12]). These compounds are extremely air-sensitive, especially in solution. Their isotropically shifted ^{1}H NMR spectra[4] are very responsive to even slight extents of oxidation, and were used to establish that all compounds subject to the measurements below were fully reduced. Solvate composition of the samples before use was checked by integration of acetonitrile vs cation or thiolate NMR signals.

Physical Measurements. All measurements were performed under strictly anaerobic conditions. Magnetic susceptibility and magnetization measurements at applied fields of 5 kOe and up to 50 kOe, respectively, were carried out on a SHE 905 SQUID magnetometer operating between 1.8 and 300 K. Magnetization experiments at 1.31 and 4.22 K employing fields up to 200 kOe were executed with a vibrating sample magnetometer (VSM).[24] Finely ground polycrystalline samples (20–30 mg) were loaded into precalibrated containers and sealed with epoxy resin under a dinitrogen/helium atmosphere. In the SQUID runs, duplicate samples were reproducible to ±2% at all values of the applied field.[25] For the VSM runs, the raw data were normalized by calibrating to a parallel sample measured in the SQUID from 0 to 50 kOe at 4.2 K. Diamagnetic susceptibility corrections[26] were applied. Mössbauer spectra were determined with a constant-acceleration spectrometer equipped with a ^{57}Co source in a Rh matrix. Zero-field measurements were made between 4.2 and 300 K with the spectrometer operating in the time mode and the source maintained at room temperature. Magnetically perturbed spectra were obtained in longitudinally applied fields up to 80 kOe with the source and absorber at 4.2 K. Polycrystalline samples were dispersed in boron nitride powder and sealed in plastic sample holders with epoxy resin. Isomer shifts are reported relative to Fe metal at 4.2 K. EPR spectra of polycrystalline solids and 15–20 mM solutions in DMF were measured at X-band frequencies on either a Varian E-109 spectrometer or a Brüker 200 spectrometer equipped with an Oxford Instruments continuous flow cryostat.

Table I. Categories of Spin Ground States of $[Fe_4S_4(SR)_4]^{3-}$ Clusters

category	no.	compound	ref
pure spin: $S = {}^1/_2$	**1**	$(Et_4N)_3[Fe_4S_4(S\text{-}p\text{-}C_6H_4Br)_4]$	9, 11, *a*
$S = {}^3/_2$	**2**	$(Et_4N)_3[Fe_4S_4(SC_6H_{11})_4]\cdot 4MeCN$	11, *a*
	9	$(Me_4N)_3[Fe_4S_4(SPh)_4]\cdot 2MeCN$	12
	10	$(Me_4N)_3[Fe_4Se_4(SPh)_4]\cdot 2MeCN$	12
	11	$(Me_4N)_3[Fe_4S_4(S\text{-}m\text{-}C_6H_4Me)_4]$	7
	12	$(Et_4N)_3[Fe_4S_4(SCH_2\text{-}p\text{-}C_6H_4OMe)_4]$	7
physical mixture: $S = {}^1/_2 +$ $S = {}^3/_2$	**3**	$(Et_4N)_3[Fe_4S_4(SEt)_4]$	*a*
	4	$(Et_4N)_3[Fe_4S_4(SMe)_4]$	*a*
	13	$(Et_4N)_3[Fe_4S_4(SPh)_4]$	5, 7
	14	$(Me_4N)_3[Fe_4S_4(S\text{-}o\text{-}C_6H_4Me)_4]$	7
	15	$(n\text{Pr}_4N)_3[Fe_4S_4(SCH_2Ph)_4]$	5, 7
spin-admixed	**5**	$(Et_4N)_3[Fe_4S_4(SCH_2Ph)_4]$	5, 7, *a*
	6	$(Et_3NMe)_3[Fe_4S_4(SPh)_4]^b$	5, 7, *a*
	7	$(Et_4N)_3[Fe_4S_4(S\text{-}t\text{Bu})_4]\cdot MeCN^b$	*a*
	8	$(Et_4N)_3[Fe_4S_4(S\text{-}i\text{Pr})_4]^c$	*a*

[a] This work. [b] Classification tentative. [c] Unclassified; only solution properties determined.

Table II. Comparative Electronic Properties of Clusters with Pure $S = {}^1/_2$ (**1**) and $S = {}^3/_2$ (**2**) Ground States

	compound	
property	**1**	**2**
$\chi^M = C/(T - \theta)^a$		
T range, K	2.2–15	2.1–70
C, emu K/mol	0.438	1.860
θ, K	−0.29	0.44
μ_{av}, μ_B	1.87	3.86
$\|D\|$, cm^{-1}; $\|E/D\|$		1.53; 0.27
δ, mm/s	0.40, 0.48	0.44
ΔE_Q, mm/s	0.94, 2.07	0.96
Γ,^{b} mm/s	0.39, 0.39	0.40
$A_x{}^c$ (H_x,^{d} kOe)	1.888 (−139) −1.323 (97)	0.627 (−129)
A_y (H_y, kOe)	1.361 (−100) −0.739 (54)	0.207 (−44)
A_z (H_z, kOe)	1.430 (−105) −0.161 (11.8)	0.468 (−89)
η	0.28, 0.42	0.86

[a] Data (T range, C, θ, μ_{av}) for other $S = {}^3/_2$ compounds. **11**: 4.2–70, 1.883, −0.79, 3.88. **12**: 4.2–30, 1.870, −0.19, 3.87. [b] Line width. [c] Magnetic hyperfine parameters for the 14.4 keV excited state of ^{57}Fe. [d] Magnetic hyperfine field; negative hyperfine field opposes applied field.

Results

Contained in Table I are the compounds containing $[Fe_4S_4(SR)_4]^{3-}$ clusters whose properties are considered in the sections that follow. Also to be found in this table are the numerical designations of the compounds and references to any prior work dealing with their electronic properties. The set of compounds contains the heretofore uninvestigated R = alkyl clusters which have become accessible by a single-step synthesis devised in this laboratory.[10] The great majority of the data reported here are new, including several measurements of previously reported

---

(13) Meyer, J.; Moulis, J.-M. *Biochem. Biophys. Res. Commun.* **1981**, *103*, 667.

(14) Moulis, J.-M.; Meyer, J. *Biochemistry* **1982**, *21*, 4762.

(15) Moulis, J.-M.; Meyer, J.; Lutz, M. *Biochem. J.* **1984**, *219*, 829.

(16) Moulis, J.-M.; Meyer, J. *Biochemistry* **1984**, *23*, 6605.

(17) Moulis, J.-M.; Auric, P.; Gaillard, J.; Meyer, J. *J. Biol. Chem.* **1984**, *259*, 11396.

(18) Gaillard, J.; Moulis, J.-M.; Auric, P.; Meyer, J. *Biochemistry* **1986**, *25*, 464.

(19) Gaillard, J.; Moulis, J.-M.; Meyer, J. *Inorg. Chem.* **1987**, *26*, 320.

(20) Auric, P.; Gaillard, J.; Meyer, J.; Moulis, J.-M. *Biochem. J.* **1987**, *242*, 525.

(21) Lindahl, P. A.; Day, E. P.; Kent, T. A.; Orme-Johnson, W. H.; Münck, E. *J. Biol. Chem.* **1985**, *260*, 11160.

(22) Lindahl, P. A.; Gorelick, N. J.; Münck, E.; Orme-Johnson, W. H. *J. Biol. Chem.* **1987**, *262*, 14945.

(23) Hales, B. J.; Langosch, D. J.; Case, E. E. *J. Biol. Chem.* **1986**, *261*, 15301.

(24) Foner, S.; McNiff, E. J., Jr. *Rev. Sci. Instrum.* **1968**, *39*, 171.

(25) See paragraph at the end of this article regarding supplementary material available.

(26) O'Connor, C. J. *Prog. Inorg. Chem.* **1982**, *29*, 203.

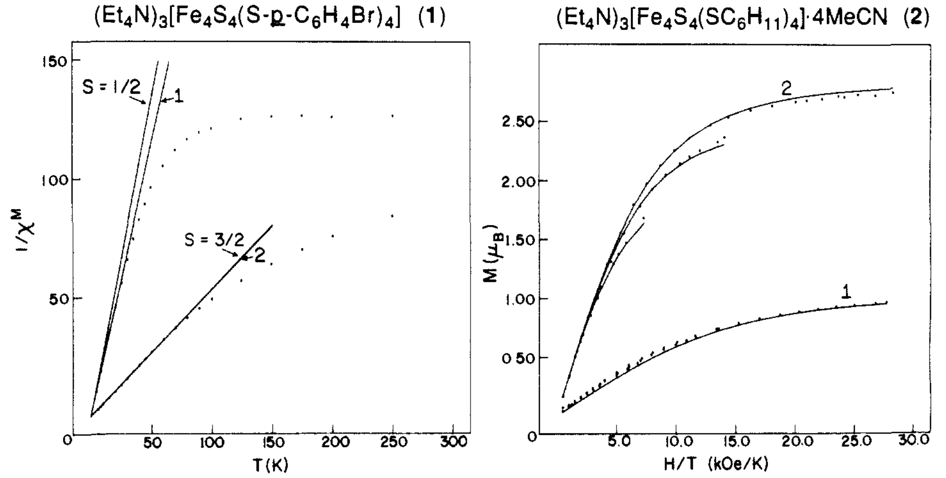

Figure 1. Magnetic properties of the pure spin clusters **1** and **2**. Left: temperature dependence of the reciprocal molar susceptibilities at $H_0 = 5$ kOe. Right: magnetization of **1** and of **2** at $H_0 = 12.5$, 25, and 50 kOe (ascending order of curves). Solid lines are calculated Curie behaviors for $S = {}^1/_2$ and ${}^3/_2$ and theoretical fits to the magnetization and low-temperature susceptibility data using the parameters in Table II.

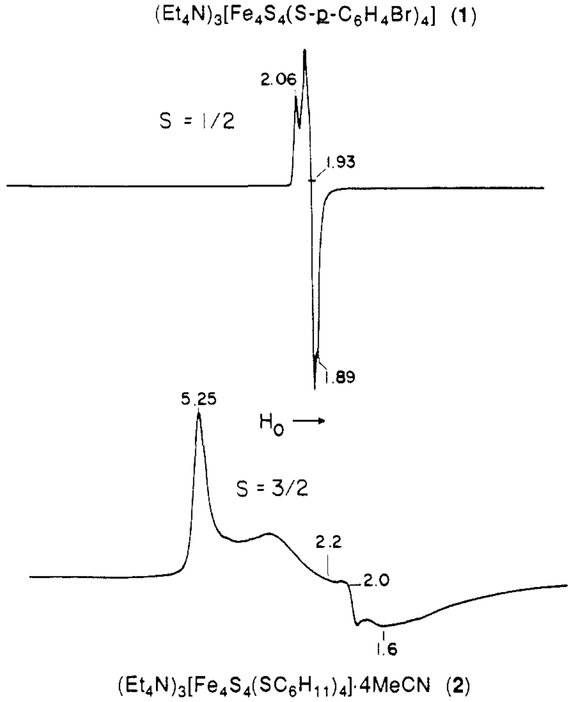

Figure 2. X-band EPR spectra of polycrystalline **1** (upper) and **2** (lower) at 7 K under the following conditions of modulation amplitude (G), microwave power (mW), and receiver gain: **1**, 25, 1.0, 16; **2**, 25, 1.0, 80. Selected g values are indicated.

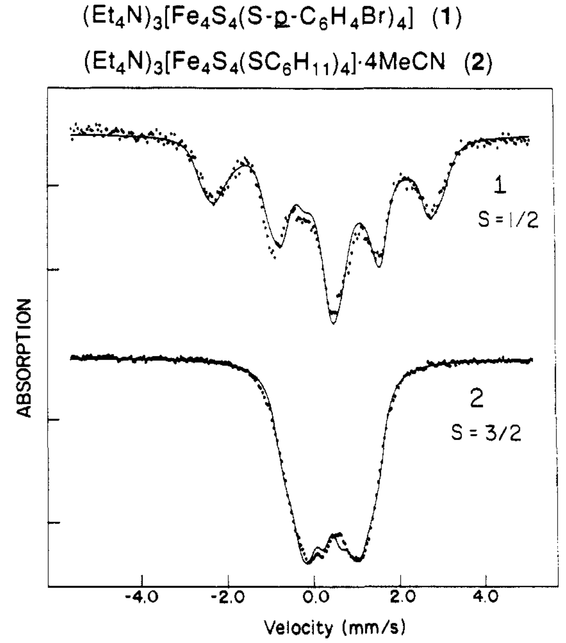

Figure 3. Mössbauer spectra at $H_0 = 60$ kOe and 4.2 K of the pure spin clusters **1** ($S = {}^1/_2$, upper) and **2** ($S = {}^3/_2$, lower). Solid lines are theoretical fits to the spectra using the parameters in Table II.

properties under different conditions and/or with more sensitive equipment. The means of recognizing and classifying clusters according to the types of spin ground states in Table I is the subject of this investigation.

Spin Ground States in Polycrystalline Solids. The combined magnetic susceptibility, magnetization, and Mössbauer and EPR spectroscopic properties have been utilized in determining cluster spin ground states. From these results, all of which have been obtained with polycrystalline samples, three categories of clusters have been recognized.

1. Pure Spin Clusters. A preliminary account of two such species, **1** and **2**, has been given earlier.[11] Of the many reduced clusters examined in this laboratory, *only* **1** exhibits a pure $S = {}^1/_2$ ground state. Compound **2** displays a pure $S = {}^3/_2$ ground state. The criteria for "pure spin" clusters of these types is made evident from the results in Table II and Figures 1–3.

Magnetization and magnetic susceptibility behaviors of **1** and **2** are shown in Figure 1. Both compounds follow the Curie–Weiss law $\chi^M = C/(T - \theta)$ at low temperatures with very small values of the Weiss constant θ and very different values of the Curie constant C. The latter are close to the theoretical values for $S = {}^1/_2$ (0.375) and ${}^3/_2$ (1.875 emu K/G) when $g_e = 2$. These parameters result from linear regression analysis of the data over the temperature ranges given in Table II. Deviations from Curie–Weiss behavior at higher temperatures arise from the population of excited state spin manifolds that are generated by the antiferromagnetic coupling among the iron atoms.

The magnetization of **1** is well described by a Brillouin function with $S = {}^1/_2$; consequently, data at different field strengths coincide exactly. Cluster **2** saturates at $2.8\mu_B$, somewhat below the theoretical value $g_e S\mu_B = 3\mu_B$ for $S = {}^3/_2$, because of zero-field splitting. The results for **2** at three different field strengths were least-squares fitted by calculating the spin projection along the magnetic field direction with use of the spin Hamiltonian 1; cluster spin $S = {}^3/_2$, and D and E are the axial and rhombic splitting parameters, respectively. Other symbols have their usual meanings. The ratio $|E/D|$ was estimated from the EPR spectrum and was held fixed in the fits; the only variable was D. The best fits at all values of the applied field (Figure 1) were obtained with the parameters in Table II.

$$H_e = D[S_z^2 - {}^5\!/_4 + (E/D)(S_x^2 - S_y^2)] + g_e\mu_B\vec{S}\cdot\vec{H} \qquad (1)$$

Polycrystalline **1** exhibits a rhombic EPR spectrum of the classic "g = 1.94 type" with apparent g values of 1.89, 1.93, and 2.05. These g values are essentially identical with those found for the $S = {}^1/_2$ form of a number of native clusters.[21,27,28] The spectrum of **2** (Figure 2) is entirely different. It is characterized by an intense absorption at g = 5.25, with other g values near 2.2 and 1.6; these are consistent with a $S = {}^3/_2$ ground state ($D > 0$) and $|E/D| \approx 0.27$. In interpreting this and subsequent spin quartet EPR spectra, the dependence of the g values of the component spin doublets on $|E/D|$ as computed from eq 1 by Lindahl et al.[21] is utilized.

The spectrum of **2** is similar to those of other spin-quartet synthetic clusters and has g values near those of the $S = {}^3/_2$ form of reduced *Av2*[21] (5.15, 5.8). The minority feature at $g \approx 2$ is attributed to a small amount of $S = {}^1/_2$ species arising from partially desolvated **2**. Independent EPR experiments on completely desolvated **2** (not shown) indicate that the spin state of the cluster changes upon desolvation and that this change is reflected in an increase in the relative intensity of the $g \approx 2$ ($S = {}^1/_2$) feature vs that in the $g = 5$ ($S = {}^3/_2$) region. We do not observe a clearly resolved signal due to a transition within the other doublet of the $S = {}^3/_2$ system. The low-field signal would be expected at g = 5.6; it could be overlapped by the strong, rather broad signal at g = 5.25 (Figure 2). Nevertheless, the observed resonances of **2** are consistent with $S = {}^3/_2$ and can be attributed to transitions occurring within the ground-state doublet.

Zero-field Mössbauer spectra of **1** (given elsewhere[9]) consist of two resolved quadrupole doublets I and II in a 1:1 intensity ratio with isomer shifts δ = 0.40 (I) and 0.48 (II) mm/s (Table II). These values and the quadrupole splittings ΔE_Q were acquired at 4.2 K. The isomer shifts indicate substantial electron delocalization, a property common to all reduced synthetic[5,7,9,12] and native[29] clusters. The magnetic Mössbauer spectrum of **1** (Figure 3) is also characterized by two equally intense subspectra. Subspectrum I, corresponding to the more "ferric" pair of Fe atoms, exhibits magnetic hyperfine fields that oppose the applied field ($A > 0$), while the more "ferrous" pair giving subspectrum II displays highly anisotropic hyperfine fields that enhance the applied field ($A < 0$). The solid line over the 60 kOe data is a theoretical fit employing the spin Hamiltonian 2 with $S = {}^1/_2$ and the parameters in Table II. The sum includes the pairs of Fe atoms, $g_n\mu_nI_i$ is the nuclear magnetic moment of ^{57}Fe, and H_Q is the quadrupole interaction given by eq 3 where the asymmetry parameter $\eta = (V_{xx} - V_{yy})/V_{zz}$; other symbols have their usual meanings.

$$H = g_e\mu_B\mathbf{H}\cdot\mathbf{S} + \sum_i[A(i)\cdot\mathbf{I}_i\cdot\mathbf{S} - g_n\mu_n\mathbf{H}\cdot\mathbf{I}_i + H_Q(i)] \qquad (2)$$

$$H_Q = (eQV_{zz}/12)[3I_z^2 - {}^{15}/_4 + \eta(I_x^2 + I_y^2)] \qquad (3)$$

In fitting the spectra of both **1** and **2**, a powder average was taken with random crystallite orientation being assumed in the sample. The quantization axes were taken to be those of the electric field gradients (EFG), assumed parallel at all Fe sites. The variables in each calculation were the signs of the principal component of the EFG (V_{zz}), η, and the magnetic hyperfine coupling constants A_x, A_y, and A_z. The 60-kOe spectrum of **1** is essentially identical with that of the $S = {}^1/_2$ form of reduced *Av2*[21] and is also very similar to the 60-kOe spectra of the $S = {}^1/_2$ [4Fe-4S]$^+$ clusters in *B. stearothermophilus* Fd[29] and *E. coli* sulfite reductase.[30]

The zero-field spectrum of **2** is sufficiently similar to those of **9** and **10**[12] that it is not shown. It is distinguished from $S = {}^1/_2$ spectra by a greater degree of apparent equivalence of the Fe atoms. The isomer shift is intermediate between those of the "ferrous" and "ferric" pairs in $S = {}^1/_2$ spectra and the quadrupole splitting is relatively small (ca. 1 mm/s). The 60-kOe spectrum of **2** in Figure 3, which is completely unlike that of **1**, was fitted by least squares with use of the Hamiltonian 1 modified to include hyperfine interaction terms. The D and E parameters were fixed by the magnetization and EPR results. The fit was performed in the limit of fast relaxation with a single set of parameters corresponding to a model having four equivalent Fe sites in the cluster. All pure $S = {}^3/_2$ synthetic clusters encountered thus far are characterized by collapsed Mössbauer spectra in large applied fields with an overall spread of about 3 mm/s and magnetic hyperfine interactions that oppose the applied field ($A > 0$, Table II). The unresolved nature of these spectra indicate near-cancellation of the applied field by the hyperfine fields at the Fe nuclei. The 60-kOe spectrum of **2** is similar in shape to those of other $S = {}^3/_2$ synthetic clusters[12] and to those of the $S = {}^3/_2$ forms of reduced *Av2*[21,22] and Se-Fd$_{red}$[20] taken in comparable applied fields.

Table III. Electronic Properties of Compounds Existing as Physical Mixture of $S = {}^1/_2$ and ${}^3/_2$ Spin States

	compound				
property	**3**	**4**	**13**	**14**	**15**
$\chi^M = C/(T - \theta)$					
T range, K	2.0–20	2.1–10	4.2–15	4.2–11	4.2–30
C, emu K/mol	1.238	0.762	0.675	1.035	1.112
θ, K	−1.16	−0.92	−1.28	−1.34	−1.60
$\lvert D\rvert$, cm^{-1}; $\lvert E/D\rvert$	4.7, 0.3	a	a	a	a
$S = {}^1/_2$, %^{b}	44	74	80	56	51
$S = {}^3/_2$, %^{b}	56	26	20	44	49

^{a} Not determined. ^{b} Estimated uncertainty from Mössbauer spectral fits is ±3%.

The magnetization, magnetic susceptibility, and Mössbauer and EPR spectroscopic properties of **9** and **10** lead unequivocally to their classification as pure spin $S = {}^3/_2$ clusters.[12] This classification for **11** and **12** is based primarily on Curie–Weiss behavior over appreciable temperature ranges with very small values of the Weiss constant (Table II).

2. Physical Mixtures of Spin States. Two representative examples of this situation are compounds **3** and **4**. Magnetic susceptibility and magnetization behaviors of **3** and the magnetic susceptibility of **4** are depicted in Figure 4. The low-temperature susceptibility of **3** in the linear region of 2.0–20 K can be accurately simulated on the basis that the sample contains 44% pure $S = {}^1/_2$ and 56% pure $S = {}^3/_2$ type clusters. The magnetization saturates at the intermediate value of 1.7μ_B, and the nested curves immediately signify the presence of a species with substantial zero-field splitting. The least-squares fit to the magnetization data corresponds also to the same 44%:56% mixture, this proportion being determined from the initial slopes of the curves. The ratio $|E/D|$ for **3** was determined from the EPR spectrum at 8 K in Figure 5, which indicates the presence of $S = {}^1/_2$ and ${}^3/_2$ clusters from the intense, nearly isotropic resonance near g = 2 and sharp feature at g = 5.3, respectively. The parameters giving the best fits to the Curie region of magnetic susceptibility and the magnetization data at all values of the applied field are summarized in Table III.

The Curie region of magnetic susceptibility of cluster **4** between 2 and 10 K (Figure 4) is consistent with a 74%:26% mixture of $S = {}^1/_2:{}^3/_2$ clusters. In addition, the initial slope of the magnetization (not shown), the apparent saturation magnetization of 1.2μ_B, the existence of nested magnetization curves at applied fields of 12.5–50 kOe, and a g = 4.7 resonance and an intense, nearly isotropic signal at g = 1.96 in the EPR spectrum (not shown) are all congruous with a mixture of $S = {}^1/_2$ and ${}^3/_2$ spin states.

Thus far we have considered the physical mixtures of **3** and **4** as consisting of $S = {}^1/_2$ and ${}^3/_2$ clusters inasmuch as these are the only pure spin states identified in the analogue clusters $[Fe_4S_4(SR)_4]^{3-}$. However, the Curie region of the susceptibility of **3** and **4** can be simulated in terms of percentages of a $S = {}^1/_2$ state and any other higher odd spin state ($S = {}^5/_2$, ${}^7/_2$, etc.). The two states just specified have been detected in reduced biological clusters.[17-20,22] Taking cluster **3** as an example, the Curie region

---

(27) Watt, G. D.; McDonald, J. W. *Biochemistry* **1985**, *24*, 7226.

(28) Bertrand, P.; Gayda, J.-P.; Rao, K. K. *J. Chem. Phys.* **1982**, *76*, 4715.

(29) Middleton, P.; Dickson, D. P. E.; Johnson, C. E.; Rush, J. D. *Eur. J. Biochem.* **1978**, *88*, 135. This paper presents a detailed analysis of a rather representative Fd$_{red}$ Mössbauer spectrum.

(30) Christner, J. A.; Münck, E.; Janik, P. A.; Siegel, L. M. *J. Biol. Chem.* **1981**, *256*, 2098.

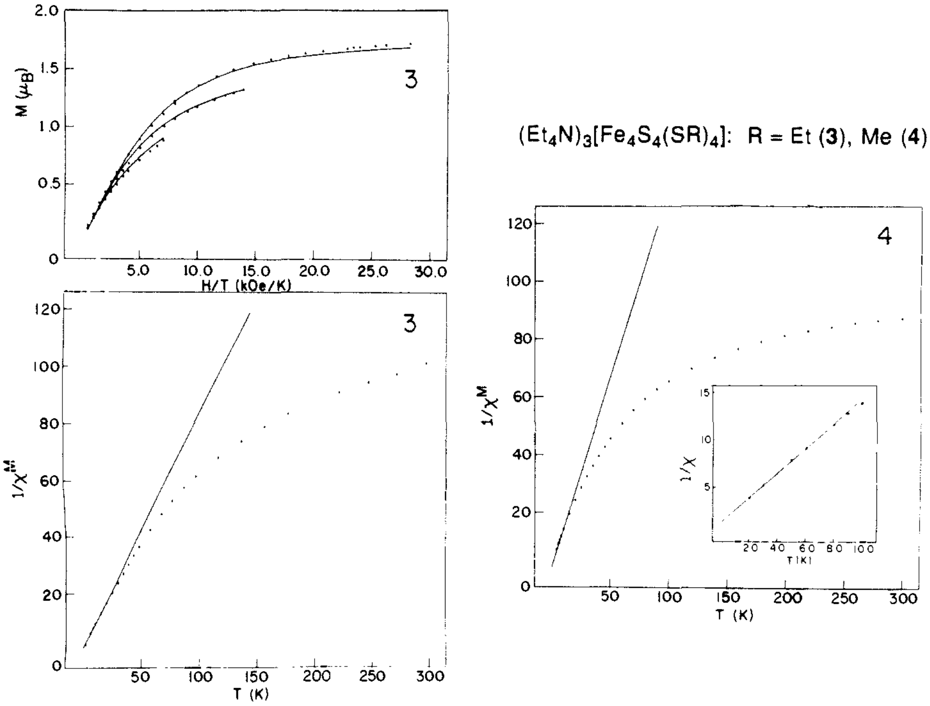

Figure 4. Magnetic susceptibility (lower) and magnetization (upper) of 3 (left) and magnetic susceptibility of 4 (right), which exist as physical mixtures of spin states. Magnetization curves in ascending order refer to H_0 = 12.5, 25, and 50 kOe; the solid lines for 3 are theoretical fits using the parameters in Table III. The straight lines are Curie–Weiss fits to low-temperature data; the inset for 4 shows the linear inverse susceptibility at 2.1–10 K measured at 100 G.

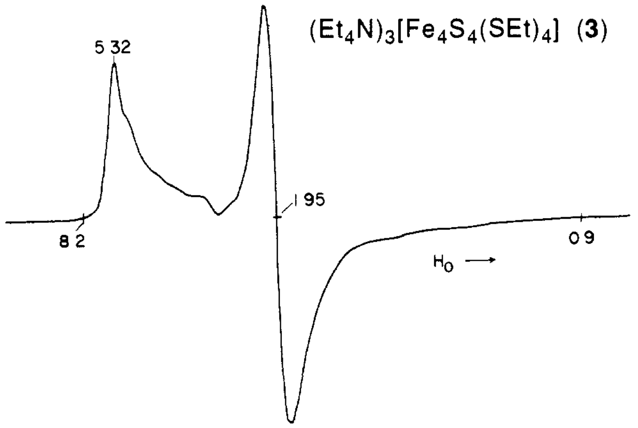

Figure 5. X-band EPR spectrum of 3 at 8 K under the conditions of 25 G modulation amplitude, 5 mW microwave power, and a receiver gain of 80; selected g values are indicated.

(C = 1.238 emu K/mol) and the initial slope of the magnetization can also be simulated by a 79%:21% $S = {}^1/_2{:}{}^5/_2$ mixture. However, fits to the entire magnetization data of 3 at all values of the applied field with these percentages are much inferior to those shown in Figure 4 and do not accurately account for the nested magnetization curves. Fits employing $S = {}^1/_2{:}{}^7/_2$ mixtures are even poorer; this result also applies to 4. In addition, the magnetic Mössbauer spectra of 3 and 4 (vide infra) cannot be adequately simulated with the larger proportions of the $S = {}^1/_2$ state necessary if one assumes the presence of $S > {}^3/_2$ states.

In the Mössbauer spectra of 3 and 4 at 60 kOe, shown in Figure 6, outer wings at +3 and −2 mm/s are clearly visible. These features are typical of the $S = {}^1/_2$ state in proteins and synthetic clusters (Figure 3). The solid line over the data points for 3 is a simulation for a 44%:56% distribution of $S = {}^1/_2{:}{}^3/_2$ clusters. This quite satisfactory fit was obtained by including a 44% contribution of a $S = {}^1/_2$ spectrum (those of 1 and reduced *Av2* gave very similar results) and allowing the remainder of the unresolved absorption in the center region to be accounted for by the $S = {}^3/_2$ contribution. Some variability in the spectra of spin quartet biological[20-22] and synthetic[12] clusters has been observed, so it is reasonable that the $S = {}^3/_2$ form of 3 may have a slightly different spectrum from these species.[31] This spectrum is also shown in Figure 6; it is in fact quite similar to, but slightly broader than,

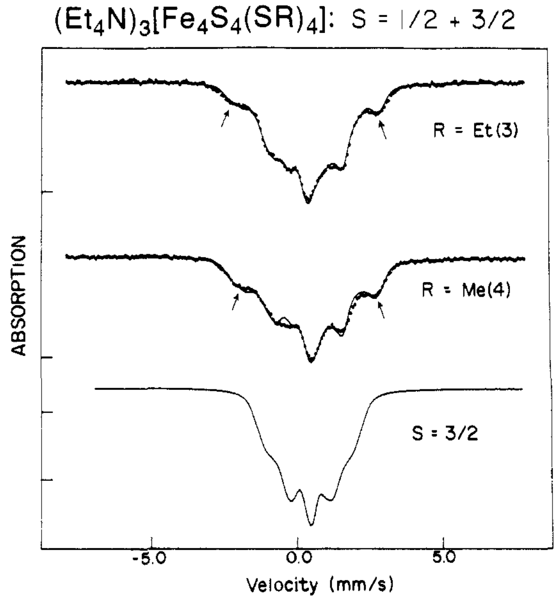

Figure 6. Mössbauer spectra at H_0 = 60 kOe and 4.2 K for 3 (upper) and 4 (middle), which exist as physical mixtures of spin states. The solid lines are theoretical fits to the data using the parameters in Table III; the $S = {}^3/_2$ component (unweighted) used in the fits is shown (lower). Arrows mark outer spectral features due to $S = {}^1/_2$ clusters.

---

[31] We have simulated the $S = {}^3/_2$ spectra of clusters 3 and 4 (as well as those of a number of compounds in frozen solution (vide infra)) using an effective $S = {}^1/_2$ Hamiltonian. The purpose here is to show the overall shape of the $S = {}^3/_2$ contribution, rather than to present a detailed analysis of these simulated spectra in terms of hyperfine parameters. It is emphasized that the percentages of the two spin states are not overly sensitive to the detailed shape of the $S = {}^3/_2$ component. The percentage of $S = {}^1/_2$ is essentially defined by the intensities of the outer wings at −2 and +3 mm/s.

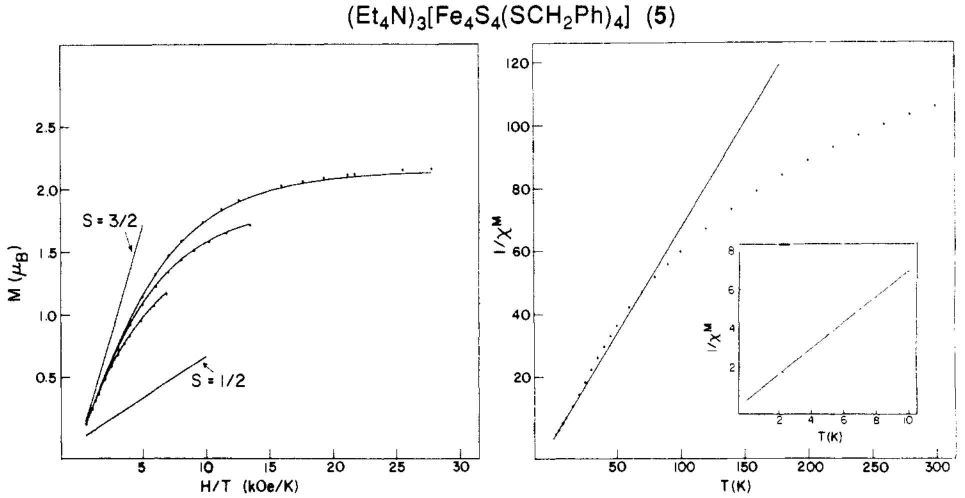

Figure 7. Magnetization (left) and magnetic susceptibility (right) of **5**. Magnetization curves in ascending order refer to H_0 = 12.5, 25, and 50 kOe; solid lines are fits to the data (see text). Lines corresponding to initial slopes for $S = {}^1/_2$ and $^3/_2$ Curie dependencies are indicated. The insert in the susceptibility plot shows the Curie behavior at 2.0–10 K measured at 100 G. The solid line is a fit to the data using the parameters in Table IV.

Table IV. Electronic Properties of "Spin-Admixed" Cluster **5**

property	
$\chi^M = C/(T - \theta)^c$	
T range, K	2.0-10
C, emu K/mol	1.497
θ, K	-0.44
δ, mm/s	0.46, 0.46
ΔE_Q, mm/s	0.86, 1.33
Γ,[a] mm/s	0.30, 0.30
H_x,[b] kOe	-70, -89
H_y, kOe	-42, -14
H_z, kOe	-57, -19

[a] Line width. [b] Magnetic hyperfine field; negative hyperfine field opposes applied field. [c] Compound **7**: 2.0–15 K, C = 1.189 emu K/mol, θ = -0.93 K.

that observed for **10**.[12] The solid line in the spectrum of **4** is a 74%:26% simulation of $S = {}^1/_2{:}{}^3/_2$ spectra, where the $S = {}^3/_2$ component was the same as used in the spectral fitting of **3**. The proportions of spin states appear to be independent of sample preparation of **3** and **4**. Separate preparations and crystallizations of these compounds afforded samples with the same magnetization curves and Mössbauer spectra. The fact that the magnetization, magnetic susceptibility, and magnetic Mössbauer results are consistent with the same spin state proportions supports the interpretation of these compounds as physical mixtures.

The identification of compounds **13**, **14**, and **15** as being physical mixtures of $S = {}^1/_2$ and $^3/_2$ states is based on combinations of magnetic susceptibility and EPR and Mössbauer spectroscopic data. Percentages of the two spin states, determined from susceptibility data in the Curie region, are also indicated in Table III.

3. "Spin-Admixed" Clusters. While certain $[Fe_4S_4(SR)_4]^{3-}$ clusters are best described as existing as a physical mixture of spin states, others that are not of the pure spin type cannot be similarly described. One such cluster is **5**, whose ambient temperature crystal structure is known[6] and whose magnetic susceptibility and Mössbauer spectroscopic properties were determined in one of our earliest investigations[5] of reduced clusters. These properties have been reinvestigated here.

The magnetization and magnetic susceptibility performance of **5** are displayed in Figure 7. Numerical data are contained in Table IV. This compound has an apparent saturation magnetization of 2.2μ_B at 1.8 K and an applied field of 50 kOe. While this situation is certainly possible for $S = {}^3/_2$ clusters, the initial slope of the magnetization (Curie region) should correspond to that for a quartet state independent of the values of D and E. The initial slope of the magnetization as well as of the Curie region of susceptibility (C = 1.497 emu K/mol) are, in fact, intermediate between the values for the $S = {}^1/_2$ and $^3/_2$ states. Thus the magnetism of **5** cannot be explained in terms of any one spin state. However, the initial slopes and saturation magnetization are not necessarily inconsistent with a physical mixture. Indeed, a 25%:75% mixture of $S = {}^1/_2{:}{}^3/_2$ (D = 2.84 cm^{-1}) simulates the data quite well, as seen in Figure 7. Nonetheless, the very high field magnetization and certain other observations cannot be interpreted in terms of such a mixture.

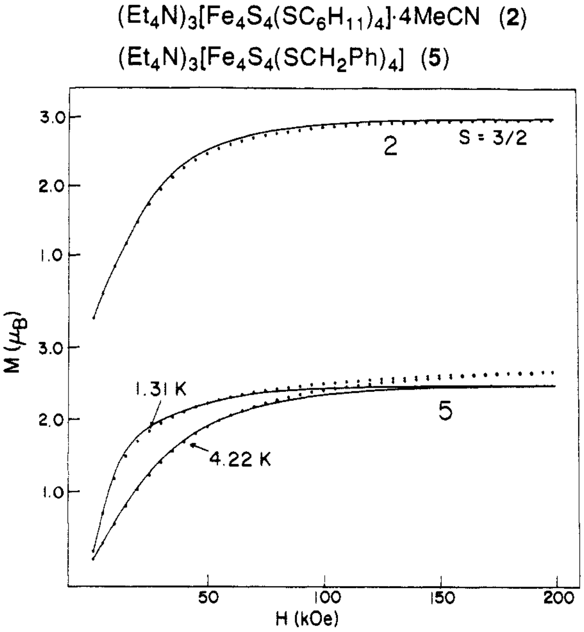

Figure 8. Magnetization of **2** at 4.22 K (upper), illustrating the behavior of a $S = {}^3/_2$ cluster, and of **5** at 1.31 and 4.22 K (lower). For **2**, the solid line is a theoretical fit to the data using the parameters in Table II. For **5**, the solid lines are attempted fits based on physical mixtures of $S = {}^1/_2$ and $^3/_2$ states (see text).

The magnetization of **5** at 1.31 and 4.22 K in fields up to 200 kOe is shown in Figure 8. Presented for comparison are the results for pure $S = {}^3/_2$ cluster **2**, which can be fit quite adequately in the expanded region of applied magnetic field by the D and E/D parameters in Table II. Note that this cluster saturates at 3.0μ_B whereas **5** closely approaches apparent saturation at 2.6μ_B and 200 kOe at both temperatures. Simulations of both the 1.31 and 4.22 K data using the parameters that afforded satisfactory fits to the results obtained at fields up to 50 kOe (Figure 7) are inadequate. The saturation magnetization value is too low in both cases. Further extensive simulations of the high-field data lead to the conclusion that the magnetization behavior over the *entire range* of applied magnetic field cannot be reproduced by a model

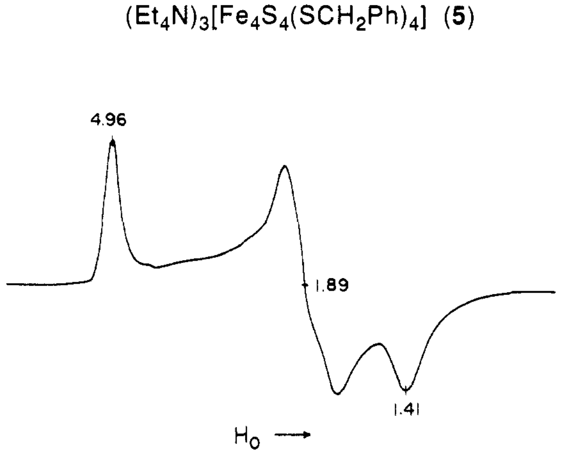

Figure 9. X-band EPR spectrum of **5** at 4.5 K under the conditions of 10 G modulation amplitude, 40 db microwave power, and a receiver gain of 800; selected *g* values are indicated.

based on any mixture of $S = {}^1/_2$ and $^3/_2$ states. Separate attempts to fit the high-field data assuming a mixture of pure $S = {}^1/_2$ and either $^5/_2$ or $^7/_2$ also produced poor fits, indicating that the magnetization of **5** cannot be rationalized in terms of a physical mixture of any pure half-integral spin states.

The low-temperature EPR spectrum of **5**, set out in Figure 9,[32] appears to be inconsistent with either a pure $S = {}^3/_2$ state or a mixture of $S = {}^1/_2$ and $^3/_2$. In particular, the apparent *g* values do not accord with a conventional $S = {}^3/_2$ system described by the Hamiltonian 1 with any value of E/D. This is most readily seen from the dependence of *g* values of the two doublets on E/D calculated by Lindahl et al.[21] For example, under the conditions $D > 0$ and $E/D = 0.18$, a resonance is predicted at $g = 4.96$ (as observed) and two others are expected at $g = 2.80$ and 1.79; these are clearly absent. The two higher field resonances actually found are at $g = 1.89$ and 1.41. We have considered the possibility that the two expected resonances are not observed because of line broadening from heterogeneities in the polycrystalline sample or level mixing (as with the $S = {}^3/_2$ form of reduced *Av2*[21]) and that the two observed signals result from some other $S = {}^3/_2$ doublet. In the latter case, a signal near $g = 1.4$ could conceivably arise from a $S = {}^3/_2$ system with either sign of D and $|E/D| \approx {}^1/_3$. However, other resonances near $g = 2.0$ and 5.5 are predicted, and neither is observed (Figure 9). We conclude that the EPR results, as the very high field magnetization behavior, cannot be interpreted in terms of a $S = {}^3/_2$ state or a physical mixture of $S = {}^1/_2$ and $^3/_2$ clusters.

The zero-field Mössbauer spectrum of **5** (not shown) can be fit with two quadrupole doublets of equal intensity and the parameters in Table IV. Magnetic Mössbauer spectra in fields of 60 and 80 kOe are provided in Figure 10. Also included in this figure is an 80-kOe $S = {}^1/_2$ spectrum scaled to 25% of the total absorption of the 80-kOe spectrum of **5**. This percentage is that which adequately simulates the magnetic susceptibility and low-field magnetization results. However, in these spectra, *the* $S = {}^1/_2$ *state signatures at +3 and −2.5 mm/s are clearly absent* (compare also with Figures 3 and 6). This observation offers persuasive evidence against cluster **5** existing as a physical mixture of $S = {}^1/_2$ and $^3/_2$ spin states. The outer wings of the 80-kOe spectrum extend out only to +1.5 and −1.0 mm/s. The spectral changes upon passing from 60 to 80 kOe are somewhat like those of pure $S = {}^1/_2$ clusters (inward- and outward-moving components), but the spectra are much more collapsed toward the center. Because we do not have an adequate model to describe the spin in large applied fields for this category of cluster, we analyzed the magnetically perturbed Mössbauer spectra of **5** by least-squares fitting using the spin Hamiltonian 2 with an effective spin $S = {}^1/_2$ to extract the magnetic hyperfine fields. The fit is shown in Figure 10 and the hyperfine fields obtained therefrom are listed in Table IV.[33] The magnetic spectra provide the strongest evidence that **5** does not belong to the preceding two categories of clusters, but is representative of a third. Further, **5** is not an isolated case; the properties of clusters **6** and **7**, while not as decisive, tend to place them in this category. Supporting data are not presented here but are available elsewhere.[34] We denote this category as "spin-admixed" inasmuch as its members display properties that do not correspond to a pure spin ground state or to physical mixtures of such states.

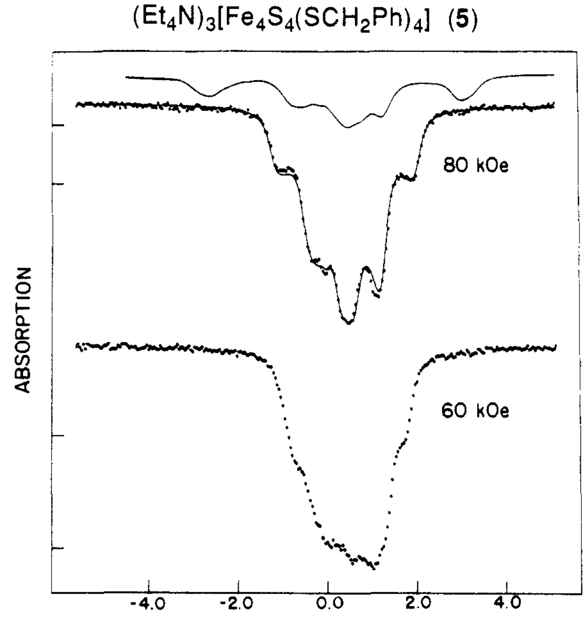

Figure 10. Mössbauer spectra of **5** in applied fields of 80 kOe (upper) and 60 kOe (lower). The solid line is a theoretical fit to the 80-kOe data using the parameters in Table IV. The solid line above the 80-kOe spectrum is a 25% contribution of an 80-kOe $S = {}^1/_2$ spectrum (see text).

Ground States in Solution. The clusters $[Fe_4S_4(SR)_4]^{3-}$ (R = arene) in frozen solution were previously shown to have practically identical zero-field and magnetic Mössbauer spectra and EPR spectra.[7] The latter are of the "$g = 1.94$ type" and resemble those of native doublet state clusters but have a smaller or zero rhombic component. The overall shape of the Mössbauer spectra is also very similar to those of the native clusters. These properties emphasize the useful analogue nature of the synthetic clusters. For both these and the native clusters, the information available until recently[11,21] indicated a $S = {}^1/_2$ ground state in frozen solution. As will be shown, reduced clusters in frozen solution are best interpreted as physical mixtures of pure $S = {}^1/_2$ and $^3/_2$ species. Nine clusters, **2**–**10**, were examined in reaching this conclusion.

EPR spectra of **2**–**8** and **10** in frozen DMF solutions at 7 K are shown in Figure 11. *All* clusters exhibit resonances in *both* the $g = 2$ ($S = {}^1/_2$) and $g = 5$ ($S = {}^3/_2$) regions. Indeed, examination of previously published spectra of $[Fe_4S_4(S\text{-}p\text{-}C_6H_4Me)_4]^{3-}$ and **12**[7] reveals weak resonances near $g = 5$ that were not interpreted at the time. The $g = 2$ regions, containing axial features with *g* values of 1.92–1.94 and 2.03–2.05, are practically identical for all the spectra. Among native clusters, these regions are very similar to the spectrum of reduced ATP-bound *Av2* ($g = 1.92$, 2.04).[22,27] Signals in the $g = 5$ region tend

---

(32) The EPR spectrum of **5** is similar to, but better resolved than, that reported earlier,[7] which appears to have been measurement at a temperature higher than that stated (4.2 K).

(33) The spectral fit shows that the data can be interpreted in terms of a 1:1 Fe subsite ratio with anisotropic hyperfine fields that oppose the applied field at both subsites. The outward-moving spectral components upon passing from an applied field of 60 kOe to one of 80 kOe arise because the hyperfine fields of the "outer" subsite are smaller in absolute magnitude than the applied field, resulting in an increase in effective (observed) field as the applied field is increased.

(34) Carney, M. J. Ph.D. Thesis, Harvard University, 1988.

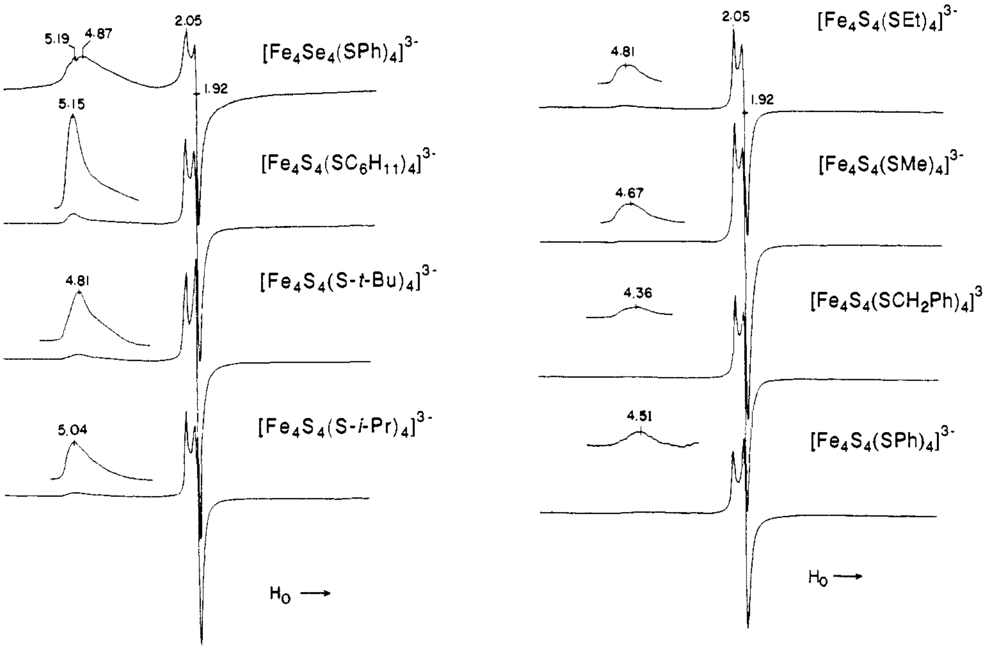

Figure 11. X-band EPR spectra of 15–20 mM solutions of clusters **2–8** and **10** in DMF at 7 K acquired with a modulation amplitude of 25 G and a microwave power of 5 mW with the following receiver gains: 125 (**2–5**, **7**), 160 (**6**), and 200 (**8**, **10**). Apparent g values are indicated; those for **3** and **10** in the $g = 2$ region are typical of the set.

Table V. Spin-State Distributions of $[Fe_4S_4(SR)_4]^{3-}$ Clusters in Frozen DMF Solutions

R	$S = {}^1/_2$, %	$S = {}^3/_2$, %
C_6H_{11} (**2**)	10	90
t-Bu (**7**)	32	68
Et (**3**)	44	56
CH_2Ph (**5**)	48	52
Me (**4**)	50	50
Ph (**6**)	56	44

to be broad and ill-resolved; their exact positions and the relative proportions of the two types of signals depend on the thiolate ligand. With Fe_4S_4 alkylthiolate clusters, the relative intensity of the $g = 5$ signal increases as, roughly, the bulk of the R group increases. We were unable to obtain accurate spin quantitations of these signals due mainly to their broadness, but the trend is evident. Of all clusters, **10** exhibits the largest proportion of $S = {}^3/_2$ form in frozen solution.

Frozen solution Mössbauer spectra of 15–20 mM solutions of clusters **2–7** in DMF at 60 and 80 kOe and 4.2 K were acquired. The spectra of four clusters at 60 kOe, presented in Figure 12, are representative of the set. They are similar but certainly not identical. All solution spectra contain features near +3 and −2 mm/s, with differing intensities, signaling the presence of varying proportions of the $S = {}^1/_2$ state. Note that **5–7** in solution (not all spectra shown) no longer exist in the spin-admixed condition. The relative proportions of $S = {}^1/_2$ and ${}^3/_2$ clusters have been quantitated by Mössbauer spectroscopy. The data were analyzed as for polycrystalline **3** and **4**. Figure 12 contains theoretical fits to the data based on the spin state percentages in Table V and the $S = {}^3/_2$ spectra used in the simulation of the experimental spectra.[31] The solubility of **10** in DMF was too low to afford a spectrum of sufficient quality for analysis.

The trend noted from the EPR results is also observed in the Mössbauer spectra: bulkier thiolates tend to favor more of the $S = {}^3/_2$ form. The relative amounts of the two spin states are about equal when the R group is relatively small, but change to 10:90 in favor of $S = {}^3/_2$ when R is cyclohexyl. Another trend is that, as the $S = {}^3/_2$ EPR resonance becomes more axial, the $S = {}^3/_2$ Mössbauer spectrum required to simulate the data becomes increasingly broadened. When R = arene (**5**, **6**) the $S = {}^3/_2$ resonance is near to $g = 4.3$ while this resonance for R = alkyl (e.g., **2** and **7**) is shifted to higher g values. Correspondingly, at 60 kOe the $S = {}^3/_2$ Mössbauer spectra for R = arene clusters are significantly broader than those for R = alkyl clusters. A similar trend has been noted for various states of reduced, nucleotide-bound *Av2*.[22]

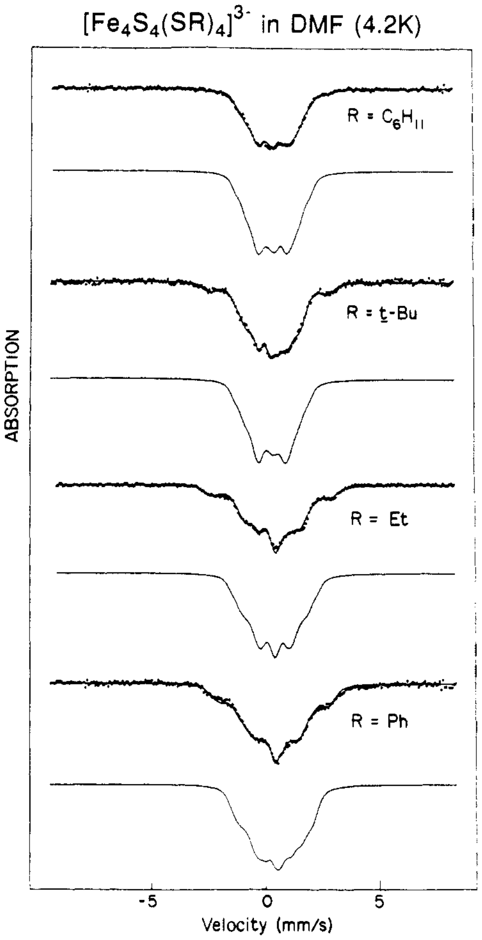

Figure 12. Mössbauer spectra of 15–20 mM solutions of clusters **2**, **3**, **6**, and **7** in DMF at 4.2 K and H_0 = 60 kOe. Solid lines through the data are theoretical fits to the data using the spin state percentages in Table V. Shown below each experimental spectrum is the $S = {}^3/_2$ spectrum (unweighted) used in the simulation.

Discussion

In our original work on spin ground states in 1979,[7] using a smaller collection of reduced clusters, we concluded that there were two cluster categories: (i) those with essentially tetragonal cores and $S = {}^{1}/_{2}$ and (ii) those with nontetragonal cores and $S > {}^{1}/_{2}$. We did not specify the spin state in the latter category, primarily because we did not achieve saturation magnetization of any member cluster.[35] Several years later, Collison and Mabbs[36] invoked the $S = {}^{3}/_{2}$ state in their analysis of powder EPR spectra of clusters in the second category, particularly **12**. This was followed by the analysis of the magnetic and Mössbauer properties of reduced *Av2* in terms of a spin state mixture,[21] and our proof in 1986,[11] based on magnetization and magnetic susceptibility of **2**, of the existence of the pure spin quartet state in a synthetic cluster. The present study has resulted in the recognition of *three* ground-state situations.

Categories of Spin Ground States. In this and prior investigations[5,7,9,11,12] we have examined the electronic properties of some 16 compounds containing 13 different reduced clusters $[Fe_4S_4(SR)_4]^{3-}$. With use of magnetization, magnetic susceptibility, and Mössbauer and EPR spectroscopic properties, we have identified the three categories of ground spin state behavior in Table I. Several of the compounds (**11**–**15**) previously studied[7] can now also be assigned to these categories.

Pure spin clusters exhibit Curie–Weiss susceptibility behavior at low temperatures with small values of the Weiss constant ($\theta < 1$ K). Two pure spin states have been identified. We now recognize that two of the compounds examined earlier, **11** and **12** (Table II), are pure spin $S = {}^{3}/_{2}$ clusters. Given the ubiquitous occurrence of native $S = {}^{1}/_{2}$ clusters with $g = 1.94$ type EPR spectra, one might expect that this state would predominate among synthetic clusters. In our sample of 16 compounds, there is only one bona fide example (**1**) of a pure $S = {}^{1}/_{2}$ ground state. With pure spin clusters, the doublet state is the exception, not the rule!

Physical mixtures of spin states are recognized by intermediate values of the Curie constant and the saturation magnetization (if achieved) and composite Mössbauer and EPR spectra containing features from these states. Of previously studied compounds,[7] the EPR spectra and the magnetic susceptibility of **13**, **14**, and **15** (Table III) lead to recognition as physical mixtures. While we cannot discount entirely clusters with odd spin states of $S > {}^{3}/_{2}$ in the mixtures, their presence is not required for a satisfactory interpretation of the magnetic and spectroscopic data.

Spin-admixed clusters ($S = {}^{1}/_{2} + {}^{3}/_{2}$) are best detected by the absence of two $S = {}^{1}/_{2}$ signatures in the wings of magnetic Mössbauer spectra and by the inability to interpret EPR spectra under Hamiltonian 1 or magnetization data to very high fields in terms of a physical mixture.

There is as yet no good theoretical description of spin-admixed cluster ground states. We note that these states may arise from the effects of unquenched orbital angular momentum. For exchange coupling of orbitally nondegenerate ions such as high-spin Fe(III), treatment under the isotropic Heisenberg exchange Hamiltonian approximation $H = \sum_{ij} J_{ij} \vec{\mathbf{S}}_i \cdot \vec{\mathbf{S}}_j$ is often successful.[37] Here and in the recent work of Münck and co-workers,[38] which includes "double exchange" to describe protein Fe_3S_4 clusters, the total spin S_T of the cluster is preserved as a good quantum number. However, for clusters composed primarily of high-spin Fe(II), such descriptions may no longer be valid because of the significant effects of orbital angular momentum. For Fe(II) in a tetrahedral site, angular momentum from the $^5T_2$ manifold can be mixed into the ground state by spin–orbit interactions. The extent of mixing will be a sensitive function of the ground and excited state energy separations, which in turn will be modulated by structural effects. Subtle structural deformations such as small Fe–S bond length changes and rotations about Fe–SR terminal bonds (resulting in different orientations of sulfur lone pair orbitals with respect to the core) can cause significant effects on orbital energies and state separations.[39,40] In those instances where orbital contributions to the magnetism cannot be treated as a perturbation, the Heisenberg Hamiltonian must be replaced by a "spin Hamiltonian" of the form[42] $H = \sum_{ij} \vec{\mathbf{S}}_i \cdot \hat{\mathbf{J}}_{ij} \cdot \vec{\mathbf{S}}_j$ where $\hat{\mathbf{J}}_{ij}$ is a general tensor that may include anisotropic and antisymmetric components and $\vec{\mathbf{S}}_j$ and $\mathbf{S}_j$ are "fictitious spins". Interactions described by this Hamiltonian yield eigenfunctions for which S_T is not a good quantum number. In a related example, spin-admixed ground states have been proposed by Maltempo[43] to describe the magnetic behavior of bacterial ferricytochrome *c′*. Recent work on related Fe(III) porphyrins suggests that the degree of admixture is dependent on changes in the axial ligand and minor geometric distortions.[44] As will be seen, $[Fe_4S_4(SR)_4]^{3-}$ clusters show a range of distortions from the highest idealized symmetry.

Irrespective of their placement in the categories above, *all polycrystalline cluster compounds when dissolved and frozen in DMF exist as physical mixtures of* $S = {}^{1}/_{2}$ *and* ${}^{3}/_{2}$ *clusters.*[45] The relative proportion of each spin state has been found to depend on thiolate substituent R, with a rough trend being increasing proportion of $S = {}^{3}/_{2}$ state with increasing steric size.[46] Cluster **10**, with a $[4Fe\text{-}4Se]^+$ core, has by far the largest percentage of quartet state among the compounds studied.

Comparisons of Synthetic and Native Clusters. The similarities in spectroscopic properties and the occurrence of $S = {}^{1}/_{2}$ and ${}^{3}/_{2}$ spin states in synthetic and biological clusters is striking. Thus, pure $S = {}^{1}/_{2}$ cluster **1** has EPR and Mössbauer spectroscopic features nearly identical with those of known $S = {}^{1}/_{2}$ protein clusters such as the ones in *Bacillus stearothermophilus* Fd_{red},[28,29] the $S = {}^{1}/_{2}$ form of reduced *Av2*,[21] and the $[4Fe\text{-}4S]^+$ center in *E. coli* sulfite reductase,[30] among others. Further, the $S = {}^{3}/_{2}$ form of reduced *Av2* in 0.4 M urea has a magnetic Mössbauer spectrum at 60 kOe applied field[21,22] that is very similar to that of pure $S = {}^{3}/_{2}$ cluster **2**, while the $S = {}^{3}/_{2}$ spectra of Se-Fd_{red} in large applied fields[20] are most like those of spin quartet clusters **9** and **10**.

Equally intriguing are the similarities in Mössbauer spectroscopic properties between synthetic clusters in frozen solution and reduced *Av2* both in its native state and under various nucleotide binding conditions. The spectrum of **7** in DMF and that of native

---

[35] In earlier work,[7] data could be obtained only up to $H/T = 13$, well short of the limits in this investigation, and the initial slopes of the curves of **5** and **12** are inconsistent with the ground-state classification above. The magnetization results in Figure 7 are to be preferred to those of our prior report.

[36] Collison, D.; Mabbs, F. E. *J. Chem. Soc., Dalton Trans.* **1982**, 1565.

[37] (a) For one application to Fe–S clusters, cf.: Girerd, J.-J.; Papaefthymiou, G. C.; Watson, A. D.; Gamp, E.; Hagen, K. S.; Edelstein, N.; Frankel, R. B.; Holm, R. H. *J. Am. Chem. Soc.* **1984**, *106*, 5941. (b) This treatment has also been applied to $[Fe_4S_4(SR)_4]^{2-,3-}$ in an initial attempt to describe antiferromagnetic exchange interactions in mixed-valence cubane clusters: Papaefthymiou, G. C.; Laskowski, E. J.; Frŏta-Pessŏa, S.; Frankel, R. B.; Holm, R. H. *Inorg. Chem.* **1982**, *21*, 1723.

[38] Papaefthymiou, V.; Girerd, J.-J.; Moura, I.; Moura, J. J. G.; Münck, E. *J. Am. Chem. Soc.* **1987**, *109*, 4703.

[39] (a) Bair, R. A.; Goddard, W. A., III *J. Am. Chem. Soc.* **1978**, *100*, 5669. (b) Ueyama, N.; Sugawara, T.; Tatsumi, K.; Nakamura, A. *Inorg. Chem.* **1987**, *26*, 1978.

[40] As one example, in reduced rubredoxin[41] the separation of the two nearest orbitals of e and t_2 parentage is about 2000 cm^{-1} or 6 kcal, an energy sufficiently small to be affected by minor structural changes.

[41] Eaton, W. A.; Lovenberg, W. In *Iron-Sulfur Proteins*; Lovenberg, W., Ed.; Academic Press: New York, 1973; Chapter 3.

[42] Lines, M. E. *J. Chem. Phys.* **1971**, *55*, 2977.

[43] Maltempo, M. M. *J. Chem. Phys.* **1974**, *61*, 2540.

[44] Gupta, G. P.; Lang, G.; Lee, Y. J.; Scheidt, W. R.; Shelly, K.; Reed, C. A. *Inorg. Chem.* **1987**, *26*, 2540.

[45] We have examined the spectroscopic properties of these clusters in acetonitrile and Me_2SO, in addition to DMF. EPR spectra in the three solvents have essentially the same relative intensities of $g \approx 2$ and 5 signals. However, the resolution in the $g \approx 2$ region is enhanced in DMF, as found in our earlier experiments.[7] Magnetic Mössbauer spectra in DMF and acetonitrile were barely distinguishable. Satisfactory Mössbauer spectra could not be obtained in Me_2SO because of the scattering effect of the solvent sulfur atoms. Watt and McDonald[27] have examined the EPR spectra of two clusters (prepared in this laboratory) in DMF solutions at 12.5 K. Signals were observed in the $g = 2$ and 5 regions. Quantitation of the former in the spectrum of **5** yielded a value (0.2–0.3 spin/cluster) that is less than the fraction of $S = {}^{1}/_{2}$ species (0.5) determined here by Mössbauer spectroscopy. The reason for this discrepancy is unclear. However, the corresponding EPR result for **2** (0.1 spin/cluster) is in agreement with the mol fraction of $S = {}^{1}/_{2}$ cluster (0.1) found in this work.

[46] Hirsh, J. *Top. Stereochem.* **1967**, *1*, 199.

Av2 in a 60 kOe parallel applied field are quite similar. In addition, the 60-kOe spectra of ADP- and ATP-bound reduced *Av2*, which have been described as being a nearly equal distribution of $S = {}^1/_2$ and ${}^3/_2$ clusters,[22] are practically identical with those of compounds **5** and **6** in frozen DMF solutions (Table V and Figure 12), in terms of both relative proportions of spin states and resolution of doublet state features at about +3 and −2 mm/s. The broadness of the $S = {}^3/_2$ spectrum of reduced *Av2*, which tends to obscure the outer wings of the $S = {}^1/_2$ spectrum, has been attributed to inhomogeneities present in the quartet species.[22] For this protein and for synthetic clusters, the appearance of a broad unresolved $S = {}^3/_2$ Mössbauer spectrum appears to correlate with a more axial $S = {}^3/_2$ EPR spectrum.

The magnetic Mössbauer spectrum at 4.2 K of the amidotransferase enzyme of *B. subtilis* is consistent with a ground state spin $S \geq {}^3/_2$.[47] The quadrupole doublet ($\delta = 0.44$ mm/s, $\Delta E_Q = 1.05$ mm/s at 100 K) of the zero-field spectrum reflects an apparent equivalence of the Fe atoms, which is strongly reminiscent of synthetic $S = {}^3/_2$ clusters. The $[4Fe-4S]^+$ centers in clostridial hydrogenase II[48] and nitrogenase Fe protein[49] also appear to have ground states with $S > {}^1/_2$, suggesting that high-spin states of native clusters are not a restrictive property.

Synthetic clusters with ground state spin $S > {}^3/_2$ have yet to be detected. Such states have been claimed for the oxidized form of the "P-clusters" of nitrogenase[50,51] ($S = {}^5/_2$ or ${}^7/_2$; assuming, as the most current evidence[52] continues to suggest, that these are $[4Fe-4S]^+$ centers), and for three Se-reconstituted ferredoxins from different organisms. These contain varying proportions of $S = {}^1/_2$, ${}^5/_2$, and ${}^7/_2$, depending on the source of the apoprotein. While the factors stabilizing these higher spin states are unknown, it is perhaps not coincidental that **10**, with its $[4Fe-4Se]^+$ core, is pure $S = {}^3/_2$ in the solid state and from EPR signal intensities has in solution the largest proportion of this state when compared to $[Fe_4S_4(SR)_4]^{3-}$ clusters (Figure 11).

The strong similarities between biological and synthetic clusters demonstrate that the latter are excellent analogues of the former in at least two spin states and support fully the spin state assignments of the protein clusters. The synthetic compounds have the attribute of unambiguous characterization. Further, the parallel trends and effects noted above, while somewhat subtle, suggest that the factors stabilizing the two spin states in synthetic and native clusters are related, at least in a phenomenological sense. As yet no protein-bound $[4Fe-4S]^+$ or $[4Fe-4Se]^+$ cluster has been shown to exist in the spin-admixed state, all such clusters being either pure spin or physical mixtures. A point to be emphasized is that when clusters are liberated from the crystal lattices of spin-admixed compounds **5**–**7** and placed in the less rigid and presumably less perturbing environment of a frozen solution, they are transformed into physical mixtures. This suggests that the spin-admixed state may be unstable with respect to the $S = {}^1/_2$ and ${}^3/_2$ states outside a crystalline environment. The total energetics of a crystal lattice may tolerate a slightly higher energy configuration of a spin-admixed $[Fe_4S_4(SR)_4]^{3-}$ cluster, something perhaps not as likely in a less rigid protein environment.

Spin State in Relation to Structure. Examination of Table I reveals that the intrinsic basicity of thiolates as measured by pK_a values[53] is not a factor in stabilizing spin states. Variation in these values can be considerable, there being a difference of ca. 3–4 between alkanethiols and benzenethiol. While the only pure spin doublet cluster contains arenethiolate ligands, the pure spin quartet, spin mixture, and spin-admixed categories contain clusters with both alkanethiolate and arenethiolate ligands.

Further inspection of Table I makes evident the pronounced influence of structural components on spin state. Thus, one can pass from pure $S = {}^1/_2$ **1** to a spin mixture **13** by changing the phenyl para substituent, from pure $S = {}^3/_2$ **11** to a mixture **14** by changing the position but not the identity of a phenyl substituent, from pure $S = {}^3/_2$ **12** to spin-admixed **5** by changing the phenyl para substituent, all with the cation constant. Alteration of cation can result in a change from a mixture **15** to spin-admixed **5** for the same cluster, and cause a given cluster to occur in all three categories (**9** (with solvate), **13**, **6**). An inevitable conclusion is that *the fine details of cluster structure and the accompanying stabilization of a ground spin state are enormously sensitive to environment.* The same is true for native clusters, with the best current example being reduced *Av2*. As already noted, the spin state proportions of this protein are strongly influenced by solvent medium and the presence of (potential) denaturants, and by nucleotide binding to the protein.

Possible Spin State/Structure Correlations. A recent EXAFS study on *Av2* led to the conclusion that the $S = {}^1/_2$ and ${}^3/_2$ states have average Fe–S bond lengths that are indistinguishable within the accuracy of the technique (±0.01 Å).[54] In the presence of Mg·ATP (known to cause pronounced EPR spectral and redox potential changes), the average bond length was unchanged. These results assure that there are no large bond length alterations accompanying the spin state change and Mg·ATP binding, but the method yields only average distances which, if nearly unchanged, would not reflect small differences in core stereochemistry. The precision of small molecule crystallography can supply such information as well as other parts of the structure. In seeking a correlation between ground spin state and cluster structure, we briefly inspect the details of the $[4Fe-4S/Se]^+$ core and the conformations of the terminal thiolate substituents. We presume that the latter property, in particular, in a crystal lattice is influenced by forces extrinsic to the core, in a manner not unlike the effect of a medium on the polypeptide binding a cluster. We state at the outset that we cannot identify a strong correlation between any one structural parameter and spin state. We submit the following considerations from data currently at hand as possible contributing factors to spin state stabilization with the caveat that electronic properties have been established at cryogenic temperatures and crystal structures at ambient temperature.

The structures of some eight reduced clusters have been determined;[5,6,9,10,12] seven of these[55] are schematically summarized in Figure 13. The latest determination is that of compound **2**. This crystal contains disordered cyclohexyl groups, cations, and solvate molecules, most of which could not be anisotropically refined. For this reason, the structure is not reported in full.[56] However, all Fe and S atoms were located and refined anisotropically, affording the Fe_4S_8 portion of the cluster whose structure and distances are contained in Table VI.

Core Fe–S/Se bonds can be divided into sets of "long" and "short", as indicated, with idealized or imposed C_2 or S_4 axes. On this basis, *four* types of core distortion from idealized cubic (T_d)

---

(47) Vollmer, S. J.; Switzer, R. L.; Debrunner, P. G. *J. Biol. Chem.* **1983**, *258*, 14284.

(48) Rusnak, F. M.; Adams, M. W. W.; Mortenson, L. E.; Münck, E. *J. Biol. Chem.* **1987**, *262*, 38.

(49) Morgan, T. V.; Prince, R. C.; Mortenson, L. E. *FEBS Lett.* **1986**, *206*, 4.

(50) (a) Huynh, B. H.; Henzl, M. T.; Christner, J. A.; Zimmerman, R.; Orme-Johnson, W. H.; Münck, E. *Biochim. Biophys. Acta* **1980**, *623*, 124. (b) Johnson, M. K.; Thomson, A. J.; Robinson, A. E.; Smith, B. E. *Biochim. Biophys. Acta* **1981**, *671*, 61. (c) Smith, J. P.; Emptage, M. H.; Orme-Johnson, W. H. *J. Biol. Chem.* **1982**, *257*, 2310. (d) Morningstar, J. E.; Johnson, M. K.; Case, E. E.; Hales, B. J. *Biochemistry* **1987**, *26*, 1795.

(51) Hagen, W. R.; Wassink, H.; Eady, R. R.; Smith, B. E.; Haaker, H. *Eur. J. Biochem.* **1987**, *169*, 457.

(52) McLean, P. A.; Papaefthymiou, V.; Orme-Johnson, W. H.; Münck, E. *J. Biol. Chem.* **1987**, *262*, 12900.

(53) (a) Jencks, W. P.; Salvesen, K. *J. Am. Chem. Soc.* **1971**, *93*, 4433. (b) Danehy, J. P.; Parameswaran, K. N. *J. Chem. Eng. Data* **1968**, *13*, 386.

(54) Lindahl, P. A.; Teo, B.-K.; Orme-Johnson, W. H. *Inorg. Chem.* **1987**, *26*, 3912.

(55) The structure of $(Me_4N)_3[Fe_4S_4(SEt)_4]$ has been determined[10] and has a compressed tetragonal core. The compound shows anomalous magnetization behavior which has not been interpreted and is too insoluble for solution measurements. For these reasons it has been incompletely studied and is not included in Figure 13.

(56) X-ray diffraction data were obtained as previously described[12] with Mo Kα radiation. Compound **2** crystallizes in monoclinic space group $P2/n$ (No. 13) with $a = 11.767$ (3) Å, $b = 15.569$ (4) Å, $c = 20.578$ (4) Å, $\beta = 102.82$ (2)°, and $Z = 2$. From 2622 unique data ($3° \leq 2\theta \leq 45°$, $I > 3\sigma(I)$), the structure was solved with a combination of direct methods (MULTAN) and Fourier techniques (CRYSTALS). Anisotropic refinement of Fe and S atoms (not disordered) and ordered C and N atoms converged at R (R_w) = 8.3% (11.0%).

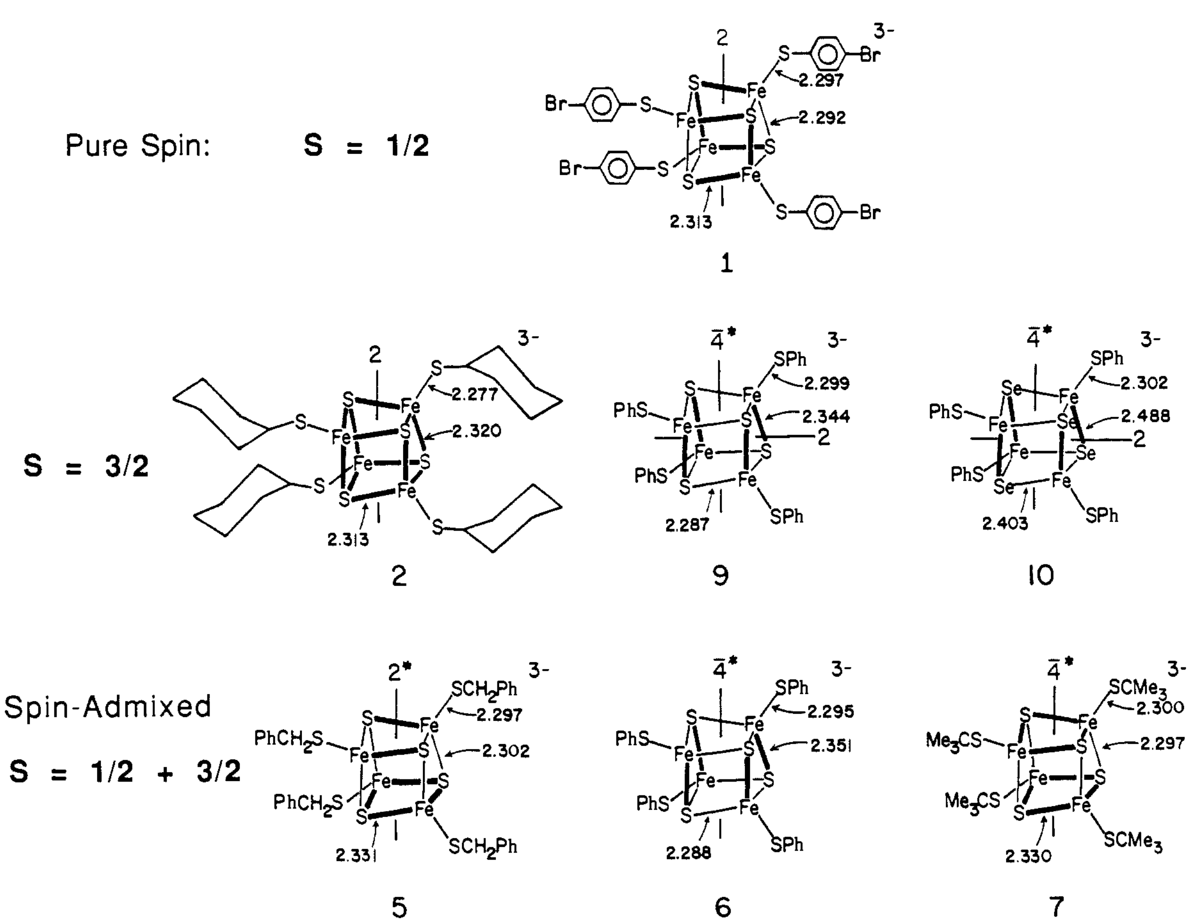

Figure 13. Schematic depictions of the cluster structures of compounds **1**,[9] **2**, **5**,[6] **6**,[5] **7**,[10] and **9** and **10**[12] arranged according to the spin state classification in Table I. Mean values (Å) of short and long (bold line) Fe–S core bonds and Fe–S terminal bonds and crystallographically imposed and idealized (*) symmetry axes are given.

symmetry are evident. Cluster **7** has a compressed tetragonal core[57] (8 long + 4 short) whereas **6** (in two different crystalline environments), **9**, and **10** show elongated tetragonal cores (4 long + 8 short). Clusters **1** and **5** exhibit less regular core distortions, with the indicated 6 long + 6 short arrangements. Because of the relatively small bond distance differences, **1** can also be described as 8 long + 4 short (compressed tetragonal). Cluster **2** is the only reduced species in which no core bond is shorter than 2.30 Å (mean 2.320 (9) Å); it may be considered to contain 12 "long" bonds. These collective results accentuate an unmistakeable stereochemical "softness" or "plasticity"[58] of the reduced core as it responds to extrinsic forces. They do not afford a relationship to spin state behavior.

One aspect of structural differences between $S = {}^1/_2$ and ${}^3/_2$ clusters is manifested in quadrupole splittings in Mössbauer spectra. Cluster **1** has two clearly resolved doublets with ΔE_Q = 0.94 and 2.07 mm/s whereas clusters with $S = {}^3/_2$ have (nearly) equivalent Fe sites by this technique with relative small quadrupole splittings of ca. 1 mm/s (Table II). This differentiation appears to hold for protein sites as well.[21,47] Xα calculations on $[Fe_2S_2(SH)_4]^{2-,3-}$ indicate a dependence of quadrupole splitting on thiolate conformation.[59] Extended Hückel calculations on $[Fe(SMe)_4]^-$ suggest that ligand orientation may influence orbital energies and Fe–S bond lengths.[39b] Because of these findings, ligand conformations of the clusters in Figure 13 were examined.

Each cluster has three torsional angles (**16**, X–Fe–S–C$_\alpha$, X = core S, Se) at each Fe subsite. When one of these angles is 180°, the thiolate substituent is placed as far from the core Fe–X edges as possible, i.e., in a staggered position. We note that $S = {}^1/_2$ cluster **1** has two angles each of 146° and 168° and that $S = {}^3/_2$ clusters **2** (173°, 176°), **9** (158°, 175°), and **10** (169°, 179°), each of twofold symmetry, have one or both angles that approach the staggered limit. In **1** the smaller angle corresponds to moving a thiolate ligand nearer to and nearly eclipsing a Fe–X bond. This effect appears to be alleviated somewhat by an opening of the Fe–S–C angle by about 5°. The Fe–SR bond of the eclipsed thiolate (2.284 (9) Å) is shorter than that of the nearly staggered thiolate (2.313 (8) Å). However, pure $S = {}^3/_2$ cluster **10** has inequivalent Fe–SR bonds (2.287 (2), 2.317 (3) Å) even though the torsional angles are nearer the staggered limit. Spin-admixed clusters **5**–**7** have, with only two exceptions, torsional angles in the 162–180° range with the majority of values about 170°. While thiolate orientation and detailed core distortions are doubtless coupled to an extent, the observed pattern of torsional angles raises the possibility that $S = {}^3/_2$ clusters tend to have ligands with conformations near the staggered limit. Calculations based on a simple van der Waals potential using the program MODEL of the CHEMGRAF suite indicate that this is the preferred arrangement. A decision as to whether $S = {}^1/_2$ clusters are stabilized by ligand conformations of a more eclipsed nature requires more than the single example available here. A theoretical investigation at the Xα level of the effect of thiolate ligand conformation on electronic structure should prove informative. Crystal structure determi-

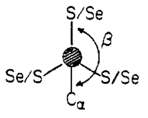

16

---

[57] Here and subsequently a dominant "tetragonal" distortion is recognized by divisions of core Fe–S bond lengths into sets of 4 + 8 under idealized D_{2d} symmetry. Not all other core structural parameters of reduced clusters necessarily follow this symmetry; those of oxidized clusters in most cases adhere rather closely to tetragonal stereochemistry. A more precise definition of tetragonal distortion in terms of shape parameters is given elsewhere.[2]

[58] Czernuszewicz, R. S.; Macor, K. A.; Johnson, M. K.; Gewirth, A.; Spiro, T. G. *J. Am. Chem. Soc.* **1987**, *109*, 7178.

[59] Noodleman, L.; Norman, J. G., Jr.; Osborne, J. H.; Aizman, A.; Case, D. A. *J. Am. Chem. Soc.* **1985**, *107*, 3418.

Table VI. Selected Interatomic Distances (Å) in the $[Fe_4S_4(SC_6H_{11})_4]^{3-}$ Cluster of Compound **2**

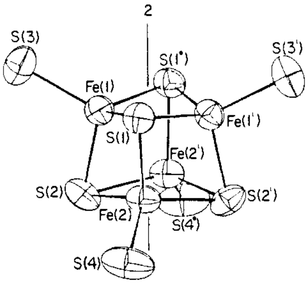

Fe(1)–Fe(1′)	2.774 (3)	Fe(1)–S(1)	2.317 (4)
Fe(1)–Fe(2)	2.774 (2)	Fe(1)–S(1′)	2.325 (3)
Fe(1)–Fe(2′)	2.783 (2)	Fe(1)–S(2)	2.323 (4)
Fe(2)–Fe(2′)	2.754 (3)	Fe(2)–S(1)	2.333 (4)
Fe(1)–S(3)	2.278 (4)	Fe(2)–S(2)	2.305 (4)
Fe(2)–S(4)	2.276 (4)	Fe(2)–S(2′)	2.318 (4)

nations at temperatures in the range of Curie magnetic behavior would appear necessary to identify the factors leading to spin state mixtures.

Solution Behavior. In our earlier investigation of reduced clusters,[7] we concluded that the probable intrinsic core structural change pursuant to electron transfer is that of reaction 4. Perturbations of this structural change would then provide one means by which protein structure could modulate potentials. At that time, reduced alkanethiolate clusters were not available and $S > {}^1/_2$ states were unproven. Present results lead to a brief reinspection of this reaction inasmuch as the existence of more than one spin state raises the matter of more than one cluster structure.

$$[4Fe\text{-}4S]^{2+} \text{ (compressed } D_{2d}) + e^- \rightleftharpoons [4Fe\text{-}4S]^+ \text{ (elongated } D_{2d}) \quad (4)$$

The compressed tetragonal description of oxidized clusters, all of which have $S = 0$ ground states, followed from the occurrence of this distortion in the crystal structures of some four oxidized clusters.[2] Since that time, seven additional $[Fe_4S_4(SR)_4]^{2-}$ structures have been acquired[60] and all show core tetragonal compression,[57] albeit to different extents. In addition, four halide and one phenoxide cluster have this arrangement;[61] there are several exceptions.[62] Given that the same type of distortion of the Fe–S core framework has been found in 16 crystals, a good case can be made that it is the inherently stable form of the oxidized core.[63] Very recently, however, Czernuszewicz et al.[58] have concluded from resonance Raman studies that $[Fe_4S_4(SCH_2Ph)_4]^{2-}$ in *N*,*N*-dimethylacetamide solution at ambient temperature has a smaller tetragonal core distortion than in the solid state and may closely approach or achieve a T_d core structure. The earlier work[7] showed that $[Fe_4S_4(SR)_4]^{3-}$ clusters (R = arene) in frozen solution had essentially identical zero-field and magnetic Mössbauer spectra which were similar in overall shapes to that of crystalline **6** (Figure 13). Under the reasonable assumption that a frozen solution is a less perturbing environment than a crystal, it was concluded that the inherently stable form of $[Fe_4S_4(SR)_4]^{3-}$ contained a tetragonally elongated core. Indeed, this geometry has since been found for two additional clusters (**9**, **10**).

We now know that all reduced synthetic clusters in frozen solution are physical mixtures of $S = {}^1/_2$ and ${}^3/_2$ states, and that the reason for the similarities in the Mössbauer spectra of arenethiolate clusters is that they exist in a ca. 1:1 mixture of spin states. This leaves two likely situations. (i) Reduced clusters have an essentially constant core structure, presumably elongated tetragonal, but in frozen solution exist in several conformational forms. These conformers are dependent on the R substituents, and a unique conformer or a related set stabilizes a given spin state. (ii) Conformations and core geometries are coupled to an extent such that there is no uniquely stable core configuration, and several or more configurations together with other structural features produce the variety of ground spin states observed for $[4Fe\text{-}4S/Se]^+$ synthetic and native clusters. In the first case the description of reaction 4 holds with possibly a small modification in the structure of the oxidized form, and in the second it does not. To take the description of this reaction further, a probe of cluster structures in solution is required. Conceivably, an analysis of resonance Raman spectra of reduced clusters in the crystalline, frozen solution, and fluid solution phases could refine the description of cluster intrinsic structural changes accompanying electron transfer.

Acknowledgment. This research was supported at Harvard University by NIH Grant GM 28856 and at MIT by the National Science Foundation. We thank Professor B.-H. Huynh for the use of EPR equipment in his laboratory and for useful discussion and Drs. E. McNiff and Y. Shapira for acquiring the high-field magnetization data.

Supplementary Material Available: Tables of atom coordinates of compound **2** and magnetic susceptibility data for reduced clusters **1–7** (8 pages). Ordering information is given on any current masthead page.

---

(60) (a) $(Me_4N)_2[Fe_4S_4(SCH_2CH_2OH)_4]$: Christou, G.; Garner, C. D.; Drew, M. G. B.; Cammack, R. *J. Chem. Soc., Dalton Trans.* **1981**, 1550. (b) $(Et_4N)_2$- and $(Me_3NCH_2Ph)_2[Fe_4S_4(S\text{-}t\text{Bu})_4]$: Mascharak, P. K.; Hagen, K. S.; Spence, J. T.; Holm, R. H. *Inorg. Chim. Acta* **1983**, *80*, 157. (c) $(Et_4N)_2[Fe_4S_4(S\text{-}p\text{-}C_6H_4NH_2)_4]$: Ollerenshaw, T. J.; Garner, C. D.; Odell, B.; Clegg, W. *J. Chem. Soc., Dalton Trans.* **1985**, 2161. (d) $(Et_4N)_2[Fe_4S_4(S\text{-}2,4,6\text{-}Me_3C_6H_2)_4]$: Ueyama, N.; Sugawara, T.; Fuji, M.; Nakamura, A.; Yasuoka, N. *Chem. Lett.* **1985**, 175. (e) $(Ph_4P)_2[Fe_4S_4(SH)_4]$: Müller, A.; Schladerbeck, N. H.; Bögge, H. *J. Chem. Soc., Chem. Commun.* **1987**, 35. (f) $(n\text{Bu}_4N)_2[Fe_4S_4(SPh)_4]$: Gloux, J.; Hendriks, H.; Rius, G. *J. Am. Chem. Soc.* **1987**, *109*, 3220.

(61) (a) $(Et_4N)_2[Fe_4S_4Cl_4]$: Bobrik, M. A.; Hodgson, K. O.; Holm, R. H. *Inorg. Chem.* **1977**, *16*, 1851. (b) $(Et_4N)_2[Fe_4Se_4Cl_4]$: Wei, C.; Liu, H.; *Jiegou Huaxue* (*J. Struct. Chem.*) **1986**, *5*, 203. (c) $(Et_4N)_2[Fe_4S_4(OPh)_4]$: Cleland, W. E.; Holtman, D. A.; Ibers, J. A.; DeFotis, G. C.; Averill, B. A. *J. Am. Chem. Soc.* **1983**, *105*, 6021. (d) $(Ph_4P)_2$- and $(Me_3NCH_2Ph)_2[Fe_4S_4I_4]$: Pohl, S.; Saak, W. *Z. Naturforsch.* **1988**, *43b*, 457.

(62) (a) $(Et_4N)_6[Fe_4S_4I_4]_2[Fe_2S_2I_4]$: Saak, W.; Pohl, S. *Z. Naturforsch.* **1985**, *40b*, 1105. (b) $(Ph_4P)_2[Fe_4S_4Br_4]$: Müller, A.; Schladerbeck, N.; Bögge, H. *Chimia* **1985**, *39*, 24.

(63) This statement is not intended to apply to clusters with mixed terminal ligands, whose rigorous core symmetry is necessarily lower than tetragonal; cf.: Kanatzidis, M. G.; Baenziger, N. C.; Coucouvanis, D.; Simopoulos, A.; Kostikas, A. *J. Am. Chem. Soc.* **1984**, *106*, 4500.